Journal of Thermal Analysis and Calorimetry, Vol. 59 (2000) 547–557

Dedicated to Prof. Edith A. Turi in recognition of her leadership in education

THERMAL ANALYSIS OF SEMI-DILUTE HYALURONAN SOLUTIONS

J. Liu and M. K. Cowman[*]

Department of Chemical Engineering, Chemistry and Materials Science, Polytechnic University
Six Metrotech Center, Brooklyn, NY 11201 USA

Abstract

The freezing and melting of water in semi-dilute (0.5–3.0%) solutions of the polysaccharide hyaluronan have been investigated by modulated differential scanning calorimetry.

High molecular weight hyaluronan inhibited nucleation of ice and significantly depressed the freezing temperature in a dynamic scan conducted at –3.0°C min^{-1}. Low molecular weight hyaluronan had a weaker and more variable effect on nucleation. The effects on nucleation, especially by the high molecular weight hyaluronan, are attributed to the influence of a hyaluronan network on the formation of critical ice nuclei.

Both high and low molecular weight hyaluronan reduced the melting temperature of ice by 0.4–1.1°C, depending on concentration. The enthalpy change associated with this transition was significantly reduced. If all of the enthalpy difference is attributed to the presence of non-freezing water, approximately 3.65 g water/g hyaluronan would be non-freezing. This result appears incompatible with published studies on hyaluronan samples of low water content. An alternative hypothesis and quantitative approach to analysis of the data are suggested. The data are interpreted in terms of a small amount of non-freezing water, and a much larger boundary layer of water surrounding hyaluronan chains, which has slightly altered thermodynamic properties relative to those of bulk water. The boundary layer water behaves similarly to water trapped in small pores in solid materials and hydrogels.

Keywords: calorimetry, hyaluronan, polysaccharides, water

Introduction

The extracellular matrix polysaccharide hyaluronan (HA) (Fig. 1) is a high molecular weight, linear polysaccharide with a repeating disaccharide covalent structure. HA is known to play an important role in tissue hydration, via its effect on interstitial osmotic pressure [1, 2]. A concentrated solution of high molecular weight HA also serves as a molecular sieve in hindering the movement of macromolecules and cells, while bulk flow

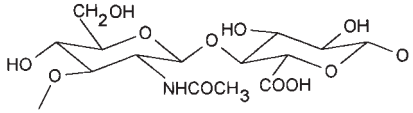

Fig. 1 Structure of the disaccharide repeat of hyaluronan

* Author for correspondence: e-mail: mcowman@duke.poly.edu

1418–2874/2000/ $ 5.00

Akadémiai Kiadó, Budapest
Kluwer Academic Publishers, Dordrecht

and diffusion of water and low molecular weight solutes are affected to a lesser degree [3, 4]. The combination of thermodynamic (osmotic) and kinetic (diffusion, flow) effects of HA on water result in the significant elastoviscosity of HA solutions. The biomechanical properties of HA solutions are of critical importance to the function of fluid tissues such as the eye vitreus and joint synovial fluid [5, 6]. They have also been utilized in the development of a series of biomedical products for use in treatment of osteoarthritic joints, as an aid to tissue manipulation and protection in eye surgery, as a protectant of the cornea in dry eye, as a means to separate tissues and minimize post-surgical adhesions, as a drug delivery vehicle, and as an additive in cryopreservation.

Despite its importance, the extent and nature of water 'binding' by HA have not been fully clarified. Strongly bound water, hydrogen-bonded to the HA structure, must be distinguished from a secondary layer of more loosely associated water, if any such structure exists as an energetically distinct entity.

The amount of strongly bound water has been investigated by adiabatic compressibility measurements on HA solutions [7, 8], and by differential scanning calorimetry (DSC) measurements of non-freezing water in hydrated HA at low water contents [9–12]. From these studies, approximately 0.6–0.7 g of water are found to be strongly bound per g HA. This corresponds to 13–16 water molecules per repeating disaccharide of HA. The level of water binding is similar to that seen for many proteins and water-soluble synthetic polymers. NMR analysis of water relaxation in HA solutions is also in accord with expectation for a low level of strongly bound water [13]. Bulk flow of water in HA solutions can be successfully modeled using a simple fiber matrix model, without need to consider specific water binding at all [14].

Additional water interactions of unknown (presumably weaker) strength are evident in other properties of HA. Quasi-elastic neutron scattering studies show a reduced mobility of bulk water in the presence of HA at concentrations of 1–8%, such that the bulk water resembles pure supercooled water [15]. 'Freezing-bound water', which freezes and melts at a lower temperature than bulk water, has been inferred to exist, based on DSC observations of HA at low water contents, in the range of approximately 0.8–3 g water/g HA (i.e., 25–56% HA) [9–12].

Recently, a much larger amount (up to approximately 2–9 g water/g HA) of apparently non-freezing water has been reported for semi-dilute (ca 1%) HA solutions, based on DSC analysis [16]. Solutions of lower HA concentration gave still higher values. In those studies, the melting endotherm of water was significantly reduced in magnitude relative to that of bulk water, and all of the difference was ascribed to non-freezing water.

In the present study, we re-examine the thermal properties of semi-dilute HA solutions. We confirm the observation of a significantly reduced magnitude for the melting endotherm, relative to that for pure water. We also note a small decrease in melting temperature. We present an alternative quantitative analysis and a hypothesis, reconciling the DSC data for lower and higher water contents, in terms of boundary layer water surrounding the HA chains. This water is suggested to be characterized by a reduced melting temperature and heat of fusion relative to that for bulk water. In this respect, the water may be considered similar to water trapped in small pores of a matrix, and thereby forced to form crystallites of reduced size. This analogy is most clear for HA at low water con-

tents, but also applies to the smaller effect seen in the boundary layer water surrounding fully solvated HA chains in semi-dilute solution.

Materials and methods

Hyaluronan (HA), isolated from *Streptococcus zooepidemicus*, was obtained from Sigma Chemical Co. (St. Louis, MO, USA). Its weight-average molecular weight was estimated by agarose gel electrophoresis [17] as $2.2 \cdot 10^6$ and also determined by low-angle laser light scattering ($M_w = 2.2 \cdot 10^6$) and capillary viscometry ($M_v = 2.1 \cdot 10^6$, based on an average of the values calculated using equations most appropriate for HA above [18] and below [19] a molecular weight of about $2 \cdot 10^6$). HA isolated from pig skin was obtained from Seikagaku Kogyo Co., Ltd. (Tokyo, Japan). Its molecular weight was estimated by capillary viscometry to be approximately $1.5 \cdot 10^5$. Both HA samples were obtained and used in the sodium salt form. HA samples were dissolved in water that had been purified by organic removal, deionized to an electrical resistance of approximately 17–18 megohm-cm, and filtered through a 0.2μm pore size membrane. The HA concentration ranged from 0.5–3.0% (w/w), and the HA solutions were slowly rotated in the cold over a period of several days to effect thorough dissolution and homogeneity.

Modulated differential scanning calorimetry (MDSC) was performed using a TA Instruments DSC 2920, equipped with a liquid nitrogen cooling accessory, and Analyst 2000 software. Samples of approximately 10 mg were placed in hermetically sealed aluminum sample pans (TA Instruments) and weighed to an accuracy of ±0.01 mg. Samples were used immediately, to avoid condensation of water on the sample pan lid, which can occur if the sealed samples are stored in the cold before use. The thermal protocols used were as follows: equilibrate at 20.0°C; isothermal at 20.0°C for 2.0 min; cool from 20.0°C to –55.0°C at 3.0°C min^{-1}, with modulation of ±0.5°C every 60 s; isothermal at –55.0°C for 2.0 min; heat from –55.0°C to 20.0°C at 3.0°C min^{-1}, with modulation of ±0.5°C every 60 s. The lower limit temperature of –55°C was chosen to ensure that all freezable water was observed. For example, it has been observed that the crystallization temperature of water can be as low as –43°C in HA/water samples of low water content.

We found the MDSC instrument to give excellent reproducibility of freezing and melting temperatures, as well as transition enthalpies. The instrumental temperature calibration constant was determined using the melting temperature of indium. As a secondary standard, we daily measured the melting temperature of ice (0.1±0.2°C, based on the indium calibration) and the apparent freezing temperature (–9±2°C, a non-equilibrium value reflecting the scan conditions and water purity). All calculations of differences in transition temperatures for HA solutions relative to pure water were based on same-day data, which increased the reproducibility of the data to about ±0.1°C for ΔT_m and ±1°C for ΔT_f. We also used water as the standard for enthalpy change. The experimental value for the melting transition, averaging 328±8 J g^{-1}, was compared to the literature value of 334 J g^{-1}, and all data for HA solutions have been normalized to a same-day water scan, assigned the value of exactly 334 J g^{-1}. The reproducibility of enthalpy values for HA so-

lutions calculated in this manner was approximately ±1%, as a result of the use of the same-day water analysis as standard.

Results and discussion

Effect of HA on freezing temperature of water

Figure 2 shows data for a representative MDSC cooling and heating curve for HA dissolved in water. The sample shown is bacterial HA at a concentration of 2.0% (w/w) in

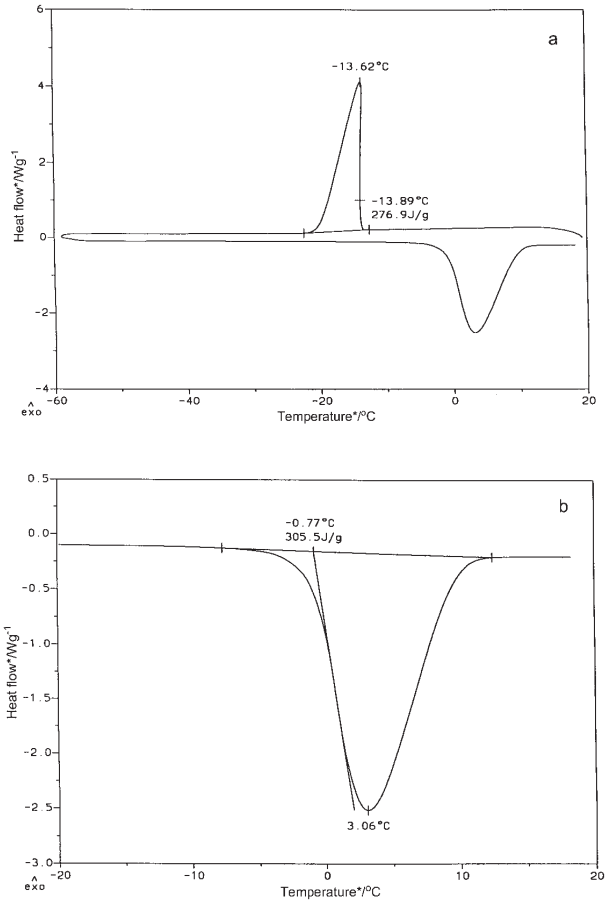

Fig. 2 a) Representative cooling and heating curves for hyaluronan solutions. The sample was bacterial hyaluronan, dissolved in water at a concentration of 2.0%. The modulated DSC scan was conducted at a rate of 3.0°C min^{-1}, with modulation of ±0.5° every 60 s. The transition temperatures and enthalpy are shown for the cooling curve
b) Expanded view of the melting endotherm portion of the MDSC curves shown in part A. The transition temperatures and enthalpy are as shown

water. The exothermic transition due to the freezing of water in the cooling curve begins at a lower temperature in the HA solution than was observed for water alone. (Under our conditions of a dynamic scan at –3.0°C min^{-1}, ice formation initiated by heterogeneous nucleation begins at approximately –9°C for pure water.) The inhibition of ice nucleation by HA solutions in this concentration range has been previously reported [20]. Table 1 gives data for a series of HA concentrations from 0.5–3.0%, for both pig skin and bacterial HA. The higher molecular weight bacterial HA has a stronger anti-nucleation effect at all concentrations. It can also be seen that the effect on nucleation changes with HA concentration, so that higher concentration can have a less inhibitory effect on ice nucleation. (Indeed, the pig skin HA at 3.0% is nucleation-enhancing.) We attribute the anti-nucleation effect to the existence of the HA network (which is less well established for the lower molecular weight pig skin HA), and its ability to inhibit formation and growth of ice nuclei, as well as to a possible specific binding of HA to nascent nuclei, limiting their growth. The opposite, nucleation-enhancing effect, which begins to show at the highest concentrations, may arise from the formation of HA aggregates, which can serve as aids to nucleation. Interestingly, the anti-nucleation activity of HA reasserts itself at even higher HA concentrations (low water content), as has previously been reported [11]. This effect is strongly reminiscent of the behavior of water trapped in small pores in silica or in hydrogels [21, 22].

Effect of HA on melting temperature of water

The heating curve shows a single endothermic transition due to the melting of ice. The onset of melting occurs at a slightly lower temperature in HA solutions than in pure water. For the 2.0% HA solution shown in Fig. 2, the difference in melting temperature (ΔT_m) was –0.8°C, measured against purified water analyzed on the same day. Table 1 lists the reduction in melting temperature seen in a series of HA solutions. The magnitude of the T_m reduction increases as HA concentration increases, but does not appear to depend on HA molecular weight. This effect is not primarily a colligative effect, since the low concentration of HA and its sodium counterions (0.025 M for a 1% HA solution) would cause only a very small freezing/melting point depression (<0.1°C)

Effect of HA on enthalpy change associated with the cooling curve

The enthalpy change associated with the cooling curve was always less than that associated with the heating curve. This is also true for water alone, and reflects the difference in heat capacity of liquid water and ice, and the need to correct the enthalpy measured at lower temperatures to the value that would be observed if the transition occurred at 0°C. For example, a 10°C difference in temperature would result in an enthalpy difference of approximately 21 J g^{-1} [21]. We observe a difference of approximately 35 J g^{-1} for water, and 29 J g^{-1} for the 2.0% HA solution in Fig. 2.

The exothermic transition due to nucleation and growth of ice in undercooled HA solutions is not an equilibrium transition, and the enthalpy change is too variable to use in determining the amount of water freezing. In addition, the variability in

Table 1 Thermal properties of hyaluronan solutions

Sample	HA conc./ g HA/100g soln	Water content/ g water/g HA	ΔT_f/ soln–water, °C	ΔT_m/ soln–water, °C	ΔH_{obs}[1]/g soln/J g^{-1}	ΔH_{obs}[1]/g HA/J g^{-1}
Pig skin HA	0.5	199	+0.5	–0.5	326.7	65 330
	1.0	99	–0.6	–0.5	317.3	31 730
	2.0	49	–1.1	–0.9	304.6	15 230
	3.0	32.3	+1.2	–1.1	283.6	9 450
Bacterial HA	0.5	199	–3.2	–0.4	325.3	65 060
	1.0	99	–3.6	–0.4	316.3	31 630
	2.0	49	–3.9	–0.8	304.6	15 230
	3.0	32.3	–0.5	–1.0	288.9	9 620

[1]Enthalpies were normalized *vs.* water sample run on the same day, assigned a value of 334 J g^{-1}.

freezing temperature in the dynamic scan would require a correction in all enthalpic data to the equilibrium freezing/melting temperature.

Effect of HA on enthalpy change associated with the heating curve

The enthalpy change (heat of fusion) associated with the heating curve is a more accurate reflection of the state of water in the HA solutions. The enthalpy correction for the <1°C difference in melting temperature for HA solutions relative to pure water is small (<2 J g^{-1}) and has been ignored here, because the accuracy of determining the difference in melting temperature is insufficient for that purpose.

The observed enthalpy change associated with melting contains no significant contribution from the heat of dilution of HA. The justification for this statement comes from two considerations. 1. We observe little or no increase in concentration of HA in the unfrozen portion of larger samples subjected to fast or slow freezing. We also observe no exclusion of HA from a moving ice front traversing a thin tube containing HA solution. 2. The reported heat of dilution [23, 24] for HA in water is very small in comparison with the enthalpy change we have recorded. For a 10 mg sample containing 1% HA, the heat of dilution would be close to 0.1 mJ, but our observed enthalpy change is on the order of 300 mJ.

Table 1 shows that the enthalpy change for melting decreases with increasing HA concentration. A common approach to analysis of such data [11, 25, 26] is to consider that there are two states for water in the sample: free water and non-freezing (*nf*) water. Only the free water contributes to the observed enthalpy change. Assuming a constant value for the enthalpy change associated with the melting of the free water (presumably similar to that for pure water), and assuming that the weight of free water is equal to the total water weight less the non-freezing water weight, the following expression holds:

$$\frac{\Delta H_{\text{obs}}}{g_{\text{HA}}} = \frac{\Delta H_{\text{free}}}{g_{\text{free water}}}\left(\frac{g_{\text{total water}}}{g_{\text{HA}}}\right) - \frac{\Delta H_{\text{free}}}{g_{\text{free water}}}\left(\frac{g_{\text{nf water}}}{g_{\text{HA}}}\right) \tag{1}$$

Thus, a plot of the enthalpy change, normalized to the polymer weight, as a function of the total water content of the sample will yield the enthalpy change for the free water as the slope. The *x*-intercept is the point at which the total water content is equal to the amount of non-freezing water, and zero enthalpy change is observed.

Figure 3 shows the result of this analysis, for HA solutions ranging in concentration from 0.5–3.0%. The slope is 334 J g^{-1}, identical to the value for bulk water. The *x*-intercept is 3.65 g water/g HA. The conventional interpretation of this result would be that there are 3.65 g non-freezing water per g HA, and this result reproduces the finding of Bettelheim and Popdimirova [16]. But such an interpretation is inconsistent with the results of a similar analysis [11] of DSC data for hydrated HA at low water contents (0.6–4 g water/g HA), which gave an *x*-intercept of 0.6 g water/g HA. Furthermore, the calculated slope is smaller for the data obtained at low water contents, being only about 312 J g^{-1} over the range of 1–4 g water/g HA. Clearly, the sim-

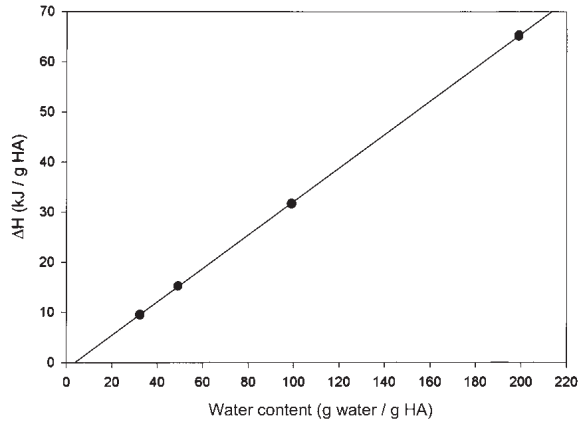

Fig. 3 Enthalpy change associated with the melting endotherm in hyaluronan solutions, normalized to the polymer weight, as a function of water content in the solution

ple data analysis described does not adequately explain the thermal behavior over a wide range of water contents.

Freezing-bound water in HA solutions

Numerous groups have described a third type of water in HA (or hylan, a chemically modified HA with enhanced molecular weight) samples at low water contents [9–12, 27]. This water, called freezing-bound water, is characterized by a lower melting temperature and a lower melting enthalpy than that of free water. It is directly observable only at water contents above 0.6 g water/g HA (or hylan) and below about 3 g water/g HA (or 10 g water/g hylan). Over this concentration range, the melting endotherm progressively moves to higher temperatures and increases in melting enthalpy. It is in all respects similar to water trapped in pores, the sizes of which increase with increasing water content. Its presence shows that HA can affect the thermodynamic behavior of several hydration layers of water. The end-point of the transition to water with properties identical to those of bulk water cannot be determined exactly, but it has been observed that water which closely approaches the same melting temperature as that of bulk water still retains a lower melting enthalpy [11, 27]. Evidence that water trapped in pores of hydrogels has an altered hydrogen-bonding structure similar to that caused by pressure increase has been found [28], so that the lower melting enthalpy would reflect a transition from ice to an altered water structure.

Consider the possibility that water in an HA solution may be of three different types: free water, freezing-bound (fb) water, and non-freezing (nf) water. Then an alternative expression can be developed for quantitative analysis of the enthalpy data, as follows:

$$\frac{\Delta H_{\text{obs}}}{g_{\text{total water}}} = \frac{\Delta H_{\text{free}}}{g_{\text{free water}}}\left(\frac{g_{\text{free water}}}{g_{\text{total water}}}\right) + \frac{\Delta H_{\text{fb water}}}{g_{\text{fb water}}}\left(\frac{g_{\text{fb water}}}{g_{\text{total water}}}\right) \tag{2}$$

This equation states that the observed enthalpy change is the weighted average of the contributions from the free water in the solution and the freezing-bound water associated with the solute; non-freezing water does not contribute. The enthalpy change may be related to the solute concentration by multiplying both sides of the equation by the water content, in g total water/g HA.

$$\frac{\Delta H_{\text{obs}}}{g_{\text{HA}}} = \frac{\Delta H_{\text{free}}}{g_{\text{free water}}}\left(\frac{g_{\text{free water}}}{g_{\text{HA}}}\right) + \frac{\Delta H_{\text{fb water}}}{g_{\text{fb water}}}\left(\frac{g_{\text{fb water}}}{g_{\text{HA}}}\right) \tag{3}$$

Expressing the weight of free water in terms of total water, freezing-bound water, and non-freezing water, we obtain:

$$\frac{\Delta H_{\text{obs}}}{g_{\text{HA}}} = \frac{\Delta H_{\text{free}}}{g_{\text{free water}}}\left(\frac{g_{\text{total water}}}{g_{\text{HA}}}\right) + \left(\frac{\Delta H_{\text{fb water}}}{g_{\text{fb water}}} - \frac{\Delta H_{\text{free}}}{g_{\text{free water}}}\right)\left(\frac{g_{\text{fb water}}}{g_{\text{HA}}}\right) - \frac{\Delta H_{\text{free}}}{g_{\text{free water}}}\left(\frac{g_{\text{nf water}}}{g_{\text{HA}}}\right) \tag{4}$$

We assume that the weight of freezing-bound and non-freezing water per g HA are constant. (Such an assumption may not be valid for very low water contents, but should hold for the semi-dilute solutions considered here.) We also assume that the enthalpic changes per g water associated with melting free water and freezing-bound water are constant. Thus, plotting the observed enthalpy change, normalized to the polymer weight, as a function of the total water content of the sample (the same x and y coordinates as previously described and used in Fig. 3), we again obtain the enthalpy change for the free water from the slope. The x-intercept, however, now includes terms for both the freezing-bound water and the non-freezing water:

$$\frac{g_{\text{nf water}}}{g_{\text{HA}}} + \left(1 - \frac{\Delta H_{\text{fb}}}{g_{\text{fb water}}}\frac{g_{\text{free water}}}{\Delta H_{\text{free}}}\right)\left(\frac{g_{\text{fb water}}}{g_{\text{HA}}}\right) \tag{5}$$

Thus, the x-intercept reflects the non-freezing water content, added to the fractional contribution of the freezing-bound water, the magnitude of which reflects the reduction in enthalpy change associated with melting of this water. For example, a 10% decrease in enthalpy change for freezing-bound *vs.* free water means the x-intercept would be increased by adding one-tenth of the weight content of freezing-bound water to the content of non-freezing water.

We can estimate the minimum amount of freezing-bound water per g HA in our solutions, by combining our data analysis with published data for HA at low water contents. Thus, the weight content of non-freezing water may be assumed to be approximately 0.6 g non-freezing water/g HA. The minimum value for the enthalpy change associated with melting the freezing-bound water is set to 312 J g^{-1}, taken from the data [11] for HA at low water contents, under conditions in which essentially all freezing water was thermodynamically affected, having a lower T_m than that of bulk water. This number is a lower limit, since it is derived from data that were not corrected for heat capacity differences at melting temperatures below 0°C. Using the

above values, and our x-intercept of 3.65, we estimate that there is at least about 44 g freezing-bound water/g HA. This value would be larger, if the average enthalpy change for melting freezing-bound water were closer to that of free water. (Note that we use an average ΔH for the freezing-bound water, but it is probable that the effect exerted by HA is distance-dependent.) If approximately 44 g of water per g HA are sufficiently strongly affected to have a lower average heat of fusion, then all of the water in an HA solution with a concentration of about 2.3% (g HA/100 g water) would be affected by the presence of the HA. The boundary layers of water surrounding nearby HA chains would effectively overlap.

An estimate of the physical dimensions of the freezing-bound water layer surrounding an HA chain can be made as follows. The volume of a disaccharide residue of HA can be determined by considering the partial specific volume of HA (ca. 0.56 $cm^3\ g^{-1}$) [29], and the disaccharide residue molecular weight of 401 for the sodium salt form, yielding 0.37 nm^3 as the volume of one disaccharide. If the disaccharide is in its most extended conformation, the length is approximately 1 nm. Thus, a circular cross-section of the cylindrical disaccharide will have an approximate radius of 0.34 nm. This is in excellent agreement with the radius (0.30±0.05 nm) measured by atomic force microscopy [30]. The water layer, containing 44 g water/g HA, contains approximately 980 water molecules per disaccharide. Assuming a density of 1 g cm^{-3}, corresponding to 33.4 water molecules per nm^3, the water layer would comprise a cylindrical shell of 29.3 nm^3 volume per disaccharide. Over the 1 nm length of the disaccharide, the thickness of the water layer would be about 2.75 nm, approximately 8 times the radius of the HA chain. This becomes effectively the boundary layer of water surrounding HA. As a comparison, it is interesting to note that if the boundary layer thickness is defined as the distance over which the relative velocity of water molecules in a flowing polymer solution reaches within 99% of that of the bulk solvent (being zero relative velocity at the polymer surface), then the boundary layer would be as much as 100 times the radius of the polymer chain. Thus, we are well within the range of distance over which the motions of the solvent are affected by the polymer.

Conclusions

Semi-dilute hyaluronan solutions have significantly altered freezing and melting transitions for water. The effects are greater than can be accounted for by the presence of a small amount of non-freezing water, strongly bound to the polymer. A larger boundary layer of water, with slightly altered thermodynamic properties, is proposed, and its size is estimated. The reduction in melting temperature and associated enthalpy change suggest that this boundary layer water behaves similarly to water trapped in small pores in solid materials and crosslinked hydrogels.

* * *

The authors wish to thank Professor Edith Turi, Polytechnic University, for encouragement, interest, and guidance in the development of this research. They also wish to thank Professors T. K. Kwei,

Shiro Matsuoka, and Kalle Levon, Polytechnic University, for helpful discussions. The DSC experiments were conducted at the Edith Turi Thermal Analysis Laboratory of the Herman F. Mark Polymer Research Institute of Polytechnic University.

References

1 W. D. Comper and T. C. Laurent, Physiol. Rev., 58 (1978) 255.
2 F. A. Meyer, Biochim. Biophys. Acta, 755 (1983) 388.
3 T. C. Laurent, 'Chemistry and Molecular Biology of the Extracellular Matrix', E. A. Balazs, Ed., Academic Press, New York 1970, pp. 703–732.
4 T. C. Laurent, Biophys. Chem., 57 (1995) 7.
5 E. A. Balazs, Fed. Proc., 25 (1966) 1817.
6 D. A. Gibbs, E. W. Merrill, K. A. Smith and E. A. Balazs, Biopolymers, 6 (1968) 777.
7 Y. Suzuki and H. Uedaira, Bull. Chem. Soc. Jpn., 43 (1970) 1892.
8 A. Davies, J. Gormally, E. Wyn-Jones, D. J. Wedlock and G. O. Phillips, Biochem. J., 213 (1983) 363.
9 H. Yoshida, T. Hatakeyama and H. Hatakeyama, 'Cellulose', J. F. Kennedy, G. O. Phillips, P. A. Williams, Eds., Horwood, Chichester, UK 1990, pp. 305–310.
10 H. N. Joshi and E. M. Topp, Int. J. Pharm., 80 (1992) 213.
11 H. Yoshida, T. Hatakeyama and H. Hatakeyama, J. Thermal Anal., 40 (1993) 483.
12 N. Jouon, M. Rinaudo, M. Milas and J. Desbrières, Carbohydr. Polym., 26 (1995) 69.
13 L. Picullel, B. Lindman and R. Einarsson, Biopolymers, 23 (1984) 1683.
14 C. R. Ethier, Biorheology, 23 (1986) 99.
15 H. D. Middendorf, D. Di Cola, F. Cavatorta, A. Deriu and C. J. Carlile, Biophys. Chem., 53 (1994) 145.
16 F. A. Bettelheim and N. Popdimirova, Curr. Eye Res., 11 (1992) 411.
17 H. G. Lee and M. K. Cowman, Anal. Biochem., 219 (1994) 278.
18 H. Bothner, T. Waaler and O. Wik, Int. J. Biol. Macromol., 10 (1988) 287.
19 E. A. Balazs, 'The Amino Sugars', Vol. 2A, E. A. Balazs and R. W. Jeanloz, Eds., Academic Press, New York 1965, pp. 401–460.
20 M. K. Cowman, J. Liu, M. Li, D. M. Hittner and J. S. Kim, 'The Chemistry, Biology, and Medical Applications of Hyaluronan and its Derivatives', T. C. Laurent, Ed., Portland Press, London 1998, pp. 17–24.
21 Y. P. Handa, M. Zakrzewski and C. Fairbridge, J. Phys. Chem., 96 (1992) 8594.
22 K. F. Arndt and P. Zander, Colloid Polym. Sci., 268 (1990) 806.
23 R. L. Cleland, Biopolymers, 18 (1979) 2673.
24 J. C. Benegas, A. Di Blas, S. Paoletti and A. Cesàro, J. Thermal Anal., 38 (1992) 2613.
25 F. X. Quinn, E. Kampff, G. Smyth and V. J. McBrierty, Macromol., 21 (1988) 3191.
26 T. W. Schenz, B. Israel and M.A. Rosolen, 'Water Relationships in Foods', H. Levine and L. Slade, Eds., Plenum Press, New York 1991, pp. 199–214.
27 S. Takigami, M. Takigami and G. O. Phillips, Carbohydr. Polym., 22 (1993) 153.
28 L. Bosio, G. P. Johari, M. Oumezzine and J. Teixeira, Chem. Phys. Lett., 188 (1992) 113.
29 A. Davies, J. Gormally, E. Wyn-Jones, D.J. Wedlock and G. O. Phillips, Int. J. Biol. Macromol., 4 (1982) 436.
30 M. K. Cowman, M. Li and E. A. Balazs, Biophys. J., 75 (1998) 2030.